

## EVIDENCE FOR MASS OUTFLOW IN THE LOW SOLAR CORONA OVER A LARGE SUNSPOT

WERNER M. NEUPERT, JEFFREY W. BROSIUS,<sup>1</sup> ROGER J. THOMAS, AND WILLIAM T. THOMPSON<sup>2</sup>

Laboratory for Astronomy and Solar Physics, NASA/Goddard Space Flight Center, Greenbelt, MD 20771

Received 1992 January 21; accepted 1992 April 1

### ABSTRACT

Spatially resolved extreme ultraviolet (EUV) coronal emission-line profiles have been obtained in a solar active region, including a large sunspot, using an EUV imaging spectrograph. Relative Doppler velocities were measured in the lines of Mg IX, Fe XV, and Fe XVI with a sensitivity of  $2\text{--}3\text{ km s}^{-1}$  at  $350\text{ Å}$ . The only significant Doppler shift occurred over the umbra of the large sunspot, in the emission line of Mg IX (at  $T_e \approx 1.1 \times 10^6\text{ K}$ ). The maximum shift corresponded to a peak velocity toward the observer of  $14 \pm 3\text{ km s}^{-1}$  relative to the mean of measurements in this emission line made elsewhere over the active region. The magnetic field in the low corona was aligned to within  $10^\circ$  of the line of sight at the location of maximum Doppler shift. Depending on the closure of the field, such a mass flow could either contribute to the solar wind or reappear as a downflow of material in distant regions on the solar surface. The site of the source, near a major photospheric field boundary, was consistent with origins of low-speed solar wind typically inferred from interplanetary plasma observations.

*Subject headings:* solar wind — Sun: corona — Sun: UV radiation — sunspots

### 1. INTRODUCTION

Although a wide range of dynamic features has been observed in the solar atmosphere at chromosphere-corona transition region temperatures ( $1 \times 10^5 < T_e < 1 \times 10^6\text{ K}$ ), from widespread downflows over quiet areas (Doschek, Feldman, & Bohlin 1976; Dere, Bartoe, & Brueckner 1986; Hassler, Rottman, & Orrall 1991) to explosive and jetlike transients in highly localized areas (Dere, Bartoe, & Brueckner 1989), possible coronal counterparts to these phenomena have remained relatively unexplored. The corona is best observed at EUV and soft X-ray wavelengths where it can be recorded without interference from photospheric radiation, and where the spatial correlation of coronal emission with underlying chromospheric and photospheric features can be reliably established. Relatively few observations of mass flows in the low corona have been made, however. Extreme ultraviolet (EUV) observations of outward velocities of up to  $15\text{ km s}^{-1}$  have been reported over coronal holes (Cushman & Rense 1978; Rottman, Orrall, & Klimchuk 1981, 1982), and upward motions of high-temperature plasma during the impulsive phase of many flares have been recorded at EUV and soft X-ray wavelengths (Cheng 1977; Antonucci et al. 1982). It is therefore of interest to examine other solar features for evidence of coronal velocity fields. In this *Letter* we report relative Doppler shift measurements of the EUV coronal emission lines of Mg IX, Fe XV, and Fe XVI made over a large sunspot, a group of smaller sunspots, and the adjacent active region. We found a significant blueshift in Mg IX over the umbra of the large spot and propose that the implied mass flow may contribute to the solar wind.

### 2. OBSERVATIONS

Near-stigmatic EUV spectra with spatial resolution of approximately  $7''$  were obtained on 1989 May 5, using an imaging spectrograph (called SERTS, for Solar EUV Rocket Telescope and Spectrograph) carried to an altitude of  $320\text{ km}$  by a Terrier-boosted Black Brant rocket. The instrument (Neupert et al. 1992) covered the spectral range from  $235$  to  $450\text{ Å}$  and provided both high-resolution spectra (typically  $60\text{--}80\text{ mÅ}$ ) over a projected line segment  $5'$  long and spectroheliograms with projected dimensions of  $5' \times 8'$ . These data were recorded on EUV-sensitive (Kodak 101-07) photographic emulsion. By co-aligning features common to both the He II ( $303.8\text{ Å}$ ) spectroheliogram recorded during the flight and a He I ( $10830\text{ Å}$ ) image obtained concurrently at the Kitt Peak National Observatory, we obtained registration to other ground-based observations to within  $5''$ . Slit jaw photographs of the solar image provided a check on the positions of sunspots and the photospheric limb relative to the spectrograph entrance aperture with  $2''\text{--}5''$  accuracy.

The principal target of the flight was NOAA region 5464, a bipolar active region centered at S18 W49 (Fig. 1a [Pl. L5]). Three EUV exposures were obtained, two of spectroheliograms of the region and one of spectra. For the spectral exposure, the payload's pointing control was programmed to position the SERTS slit over the region's large trailing sunspot. The slit jaw photographs verify that the slit passed within  $3'' \pm 5''$  of the center of the large spot and within a similar distance of a smaller group of spots farther toward the west limb in the same region.

A patrol photograph (Fig. 1b), taken in the center of H $\alpha$  at the time of the flight, shows the major features of the active region. The large spot is clearly visible (somewhat below the center of the image) as are two smaller spots  $55''$  to the west. Figure 1c is a SERTS spectroheliogram in Mg IX at  $368.1\text{ Å}$  of the same region, while Figure 1d shows the location of the experiment's entrance slit, along which stigmatic spectra were

<sup>1</sup> Postal address: Hughes STX Corporation, 4400 Forbes Boulevard, Lanham, MD 20706.

<sup>2</sup> Postal address: Applied Research Corporation, 8201 Corporate Drive, Landover, MD 20785.

obtained, superposed on a contour plot of the Mg ix spectroheliogram. The last frame also includes projected coronal magnetic field lines calculated from nearly coincident photospheric magnetogram observations using the Sakurai (1982) potential field extrapolation code.

### 3. DATA ANALYSIS

#### 3.1. Emission-Line Positions

For the present analysis we used emission lines of Mg ix (at 368.1 Å), Fe xv (at 284.2 Å), and Fe xvi (at 335.4 and 360.8 Å) that had photographic densities in the linear portion of the  $D$ -log  $E$  curve. Measurements of emission-line positions were carried out by two independent methods. Measurements were made directly on the original negatives using a Grant Series 800 comparator-microphotometer with line segments 200  $\mu$ m long (corresponding to a pixel length of 18" on the Sun) of the 3.3 mm long spectral line image. This method required visual matching of forward and reverse line profile scans displayed on a CRT. The superposition of the two traces routinely gives a precision of 1  $\mu$ m in measurement of line positions on a photographic plate. Positional data (the location of the machine's scanning table) are determined by an optical encoder on the machine's screw and transmitted directly to a computer.

Line positions were also determined by fitting Gaussian profiles to digitized data obtained with a Perkin-Elmer Model 1010M (PDS) microdensitometer scanning the entire spectrum with a 5  $\mu$ m square aperture. (FWHM widths of the emission lines were typically 35  $\mu$ m microns [80 mÅ] to 55  $\mu$ m [120 mÅ]). Measurements made with the Perkin-Elmer machine were summed into 100  $\mu$ m bins along the slit but retained as 5  $\mu$ m pixels in the spectral direction. We measured laboratory spectra of Ne II taken before and after the flight to determine the presence of any residual curvature or irregularities in the slit images and to establish the noise level in the measurements due to grain in the photographic emulsion. Deviations from a straight line for each position along the slit, as derived from the average of five calibration lines, are shown in Figure 2. Standard deviations of the means of the five calibration lines for both the PDS and Grant measurements were 0.66  $\mu$ m. The two measurement schemes gave similar results on the flight data. Only the PDS measurements were, however, used in subsequent analysis as their pixel size better matched the spatial resolution of the SERTS.

Our estimates of the precision of positional measurements were confirmed with the solar spectrum itself by measuring the differences in spectral positions of two strong Fe xvi lines at 335.4 and 360.8 Å, again using 9" increments along the slit. Because of proximity of these lines in the spectrum, any Doppler shifts should be the same within 10%, and observed fluctuations in separations should be due primarily to film grain irregularities and measurement inaccuracies. The standard deviation of separations of the two emission lines was 1.6  $\mu$ m, implying an RMS positional inaccuracy of 1.1  $\mu$ m for each individual line, a result consistent with measurements on the laboratory spectra.

The wavelengths of the coronal EUV emission lines have estimated accuracies of 4–20 mÅ (Behring et al. 1976), corresponding to line-of-sight velocity uncertainties of 4–20 km s<sup>-1</sup> at 300 Å, and no independent wavelength calibration was carried out on the SERTS instrument. Small, localized deviations from mean line positions (wavelength shifts) can therefore be expressed only as line-of-sight velocities relative to

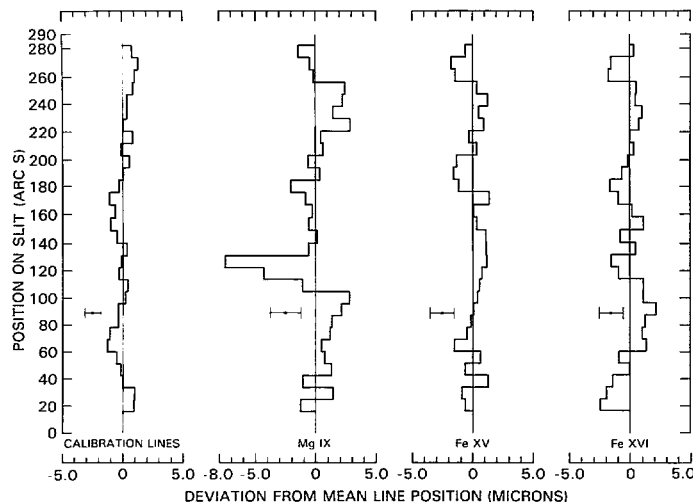


FIG. 2.—Deviations from a nominal straight line slit image for each position along the SERTS slit for the average of five calibration lines of Ne II and for coronal lines of Mg ix, Fe xv, and Fe xvi. The error bar for the calibration lines is one standard deviation ( $\pm 1 \sigma$ ) of the five-line average. For the coronal lines, the error bars represent standard deviations of measurements on individual laboratory lines comparable in density to the weakest portion of each coronal line. The major sunspot was centered at position 129, and the group of small spots was located at position 184.

a zero mean line-of-sight velocity for the active region as a whole. The slit itself covered only a small portion of the solar diameter, corresponding to a velocity differential along the slit due to solar rotation of 0.6 km s<sup>-1</sup>. This has been ignored. The average velocity of the rocket payload along the line of sight to the Sun was 0.55 km s<sup>-1</sup> during the 246 s long spectral exposure, and that has also been ignored. The changing velocity of the payload during the exposure (by 2.2 km s<sup>-1</sup>) would appear as a nominal line blurring of 2.2 mÅ (1  $\mu$ m) at 300 Å, a small effect when compared to the instrumental line width.

### 4. OBSERVATIONAL RESULTS

#### 4.1. Doppler Shifts in Coronal Lines

Figure 2 presents the measured deviations from a straight line fit of the centers of fitted Gaussian profiles for Mg ix, Fe xv, and Fe xvi along the spectrograph slit. Also indicated as an estimate of error for each solar line is the standard deviation of measurements obtained on a laboratory line whose photographic density was comparable to the weakest portion of the observed coronal line. In only one emission line, that of Mg ix at 368.1 Å, did we find any portion of the line with a wavelength shift significantly greater than the errors we have discussed above. In that case, two adjacent 9" pixels, coincident with the large sunspot within our alignment errors, exhibited wavelength shifts of 5.0 and 2.7 standard deviations from the mean position of all pixels (5.3 and 3.0 standard deviations if these two data points are not included in the mean). Measurements with both the Grant and Perkin-Elmer machines gave similar results. These displacements in wavelength corresponded to line of sight velocities of 14.3 and 8.0 km s<sup>-1</sup> toward the observer. We can find no systematic error or blemish in the photographic emulsion that would cause us to discard these particular points and must conclude that they represent actual wavelength shifts for those pixels. One cannot argue that wavelength shifts could be produced as the result of scattered light from the bright adjacent portion of the active region, for such

scatter would tend to obscure or reduce rather than emphasize a wavelength shift in the low intensity region. Measurements over the smaller sunspots showed no statistically significant Doppler shifts relative to the mean spectral position of the line. Our observations in Fe xv and Fe xvi (originating at  $2\text{--}3 \times 10^6$  K) did not show significant wavelength shifts at any location along the slit.

## 5. DISCUSSION

### 5.1. Coronal Mass Velocities Inferred from the Observations

EUV observations of the corona over the solar disk provide direct correlation with underlying photospheric features and also minimize the ambiguity arising when multiple regions of emission are observed along a single line of sight at the solar limb. Using disk observations with adequate spatial resolution, one can distinguish motions of individual features imaged along a spectrograph slit whereas, at the limb, the individual line profiles would be blended into a single, broadened profile that could mimic broadening due to turbulence. We found that relative line-of-sight velocities across the active region at spatial scales of 6000 km ( $9''$ ) or larger could be combined to produce line broadening of at most  $5 \text{ km s}^{-1}$  within a single active region. This value is far less than nonthermal velocities inferred from broadened profiles, either at the limb or on the disk. Reported nonthermal velocities range from  $10\text{--}30 \text{ km s}^{-1}$  for EUV lines produced at  $1\text{--}3 \times 10^6$  K (Feldman & Behring 1974) to as high as  $60 \text{ km s}^{-1}$  for soft X-ray lines at  $3 \times 10^6$  K in active regions (Saba & Strong 1991). In fact, excess emission-line widths, over those expected for solely thermally broadened lines, persisted in our data even at spatial scales of  $9''$ .

The region over which the blueshifted emission was recorded was one of high longitudinal photospheric magnetic field and high extrapolated coronal field (Fig. 3). The line-of-sight velocity was probably close to the actual velocity of the plasma, because the calculated potential magnetic field (for heights less than 10,000 km) was aligned to within  $10^\circ$  of the line of sight at that location. A comparable velocity was measured by Rottman et al. (1981, 1982) in an emission line of Mg x, produced at about  $1.2 \times 10^6$  K, over a coronal hole. The spatial extent of the outflow matched the foreshortened width of the spot umbra (about  $16''$ , measured along the spectrograph slit).

If the outflow occurred along field lines that returned to the Sun at distant locations, then it could be a source of mass for the downward flows in the chromosphere and transition region over the quiet Sun that have been reported by many observers. However, we did not observe statistically significant blue- or redshifted Mg ix emission in other portions of the active region that had bipolar fields and for which our potential field calculations showed closed magnetic loops. We propose an alternative explanation: that the outward flow from the sunspot umbra occurred in field lines that were open to interplanetary space. A near-radial and possibly open field in the core of the umbra is compatible with recent models of sunspot fields (Pizzo 1986; Brosius & Holman 1989) and vector field measurements (Lites & Skumanich 1990). Although we did not find any open field lines in our potential field calculations, that result may be the consequence of the finite size ( $147,000 \times 278,000$  km on the Sun) of the magnetogram used in the field calculations.

### 5.2. Comparison of the Transition Region and the Corona over Sunspots and in Coronal Holes

It is of interest to point out similarities and differences between coronal holes and sunspots, as recorded in the EUV.

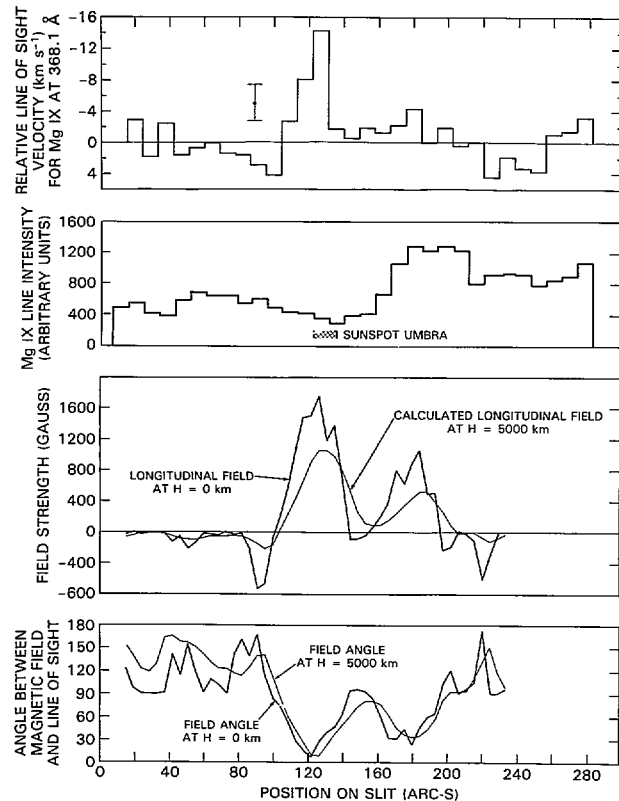


FIG. 3.—Comparison of relative velocities inferred from the Mg ix emission line at 368.1 Å with Mg ix line intensity, coronal magnetic field strength, and field angle alignment along the SERTS line of sight, as computed in a potential field approximation. The two regions of enhanced field correspond to the large sunspot and to the group of small spots traversed by the SERTS slit. The coronal field at heights less than 10,000 km was aligned to within  $10^\circ$  of the line of sight to the major sunspot.

The brightness of the transition region in the EUV is appreciably different over sunspots than below coronal holes. Transition region intensities are enhanced over sunspots, as compared to both quiet and weak plage regions (Brueckner & Bartoe 1974; Foukal et al. 1974) whereas there are no differences or possibly even small reductions in transition region intensities in holes relative to surrounding quiet regions (Brueckner & Bartoe 1974; Huber et al. 1974). Supporting this result, analyses of EUV spectra of both coronal holes (Gabriel 1976) and sunspots (Foukal et al. 1974) indicate that the transition region is 6 times (coronal holes relative to the quiet Sun) to 10 times (sunspots relative to weak plage) thicker than over active regions and that the ultimate temperature of the corona over both types of features is reduced, as compared to active regions. Thus, the transition region temperature gradient may be even lower over a large spot than over a hole. Gabriel (1976) has argued that a reduced temperature gradient in the transition region reflects the conversion of downward-conducted flux into the enthalpy requirements of an accelerating solar wind in coronal holes. His argument appears to be immediately applicable to any open field regions above the umbra of a large sunspot.

Another similarity between coronal holes and the corona over large sunspots is their diverging magnetic field geometry. For holes, this was initially pointed out by Altschuler, Trotter, & Orrall (1972). The increasing size of enhanced transition region emission with temperature over a sunspot (Foukal et al. 1974) and the orientation of coronal loops near a sunspot

observed at the limb (Beckers & Schneeberger 1974) imply a divergent field over sunspots. The divergence of the field over the large spot that we observed is clearly evident in the calculated field lines of Figure 1d. The diverging field over a coronal hole has been shown to lead to high expansion velocities near the coronal base (Holzer 1977), and similar circumstances may be present over a sunspot umbra.

Parker (1974) has proposed that a sunspot could be a region of enhanced rather than inhibited energy transport and that such a region might generate "copious fluxes of hydro-magnetic waves, which propagate out of the region along the magnetic field." Although the upward-moving waves are likely to be strongly reflected (Uchida & Kaburaki 1974; Beckers & Schneeberger 1977), the mechanical wave flux in the corona over a sunspot can nevertheless be as high as  $4 \times 10^7$  ergs  $\text{cm}^{-2} \text{s}^{-1}$  (Beckers & Schneeberger 1977). This flux level would be more than adequate to drive the solar wind in a coronal hole (Parker 1986) and, hence, in open magnetic fields over a sunspot umbra.

### 5.3. Possible Association of a Sunspot Wind with the Low-Speed Component of the Solar Wind

Several authors (see Gosling et al. 1981 and references therein) have mapped interplanetary low-speed wind events back to a coronal source surface that tracks the magnetic

neutral line of a coronal streamer belt encircling the Sun. This neutral line in turn matches the magnetic neutral line separating photospheric regions of opposite magnetic polarity (Hakamada 1987). The sunspot we observed was within  $30^\circ$  of an inversion line of the source surface field and within  $10^\circ$  of a major photospheric field boundary, as reported by the Wilcox Solar Observatory (Solar Geophysical Data 1989). Its location is therefore not inconsistent with its being a possible source for the low speed component of the solar wind. The correspondence with low-speed wind events detected by *IMP 8* is inconclusive, possibly due to the  $14^\circ$  latitude difference between the sunspot and the spacecraft.

We wish to recognize the contributions made by the staffs at the Big Bear Solar Observatory, Kitt Peak and Sacramento Peak Observatories of the National Solar Observatories, NOAO, the Goddard Space Flight Center's Southwest Station at Kitt Peak, the Observatoire de Paris at Meudon, and NOAA's Space Environment Laboratory (Boulder) in supporting our rocket launch activities with correlative observations. We are also indebted to L. Cohen and D. Klinglesmith for their support in densitometry and measurement of the flight records. This work was supported under NASA RTOP 879-11-38.

### REFERENCES

- Altschuler, M. D., Trotter, D. E., & Orrall, F. Q. 1972, *Sol. Phys.*, 26, 354  
 Antonucci, E., et al. 1982, *Sol. Phys.*, 78, 107  
 Beckers, J. M., & Schneeberger, T. J. 1977, *ApJ*, 215, 356  
 Behring, W. E., Cohen, L., Feldman, U., & Doschek, G. A. 1976, *ApJ*, 203, 521  
 Brosius, J. W., & Holman, G. D. 1989, *ApJ*, 342, 1172  
 Brueckner, G. E., & Bartoe, J.-D. F. 1974, *Sol. Phys.*, 38, 133  
 Cheng, C.-C. 1977, *Sol. Phys.*, 55, 413  
 Cushman, G. W., & Rense, W. A. 1978, *Sol. Phys.*, 58, 299  
 Dere, K. P., Bartoe, J.-D. F., & Brueckner, G. E. 1986, *ApJ*, 305, 947  
 ———. 1989, *Sol. Phys.*, 123, 41  
 Doschek, G. A., Feldman, U., & Bohlin, J. D. 1976, *ApJ*, 205, L177  
 Feldman, U., & Behring, W. E. 1974, *ApJ*, 189, L45  
 Foukal, P. V., et al. 1974, *ApJ*, 193, L143  
 Gabriel, A. H. 1976, in *The Energy Balance and Hydrodynamics of the Solar Chromosphere and Corona*, ed. R. M. Bonnet & Ph. Delache (Clermont-Ferrand: G. de Bussac), 375  
 Gosling, J. T., Borrini, G., Asbridge, J. R., Bame, S. J., Feldman, W. C., and Hansen, R. T. 1981, *J. Geophys. Res.*, 86, 5438  
 Hakamada, K. 1987, *J. Geophys. Res.*, 92, 4339  
 Hassler, D. M., Rottman, G. J., & Orrall, F. Q. 1991, *Adv. Space Res.*, 11(1), 141  
 Holzer, T. E. 1977, *J. Geophys. Res.*, 92, 23  
 Huber, M. C., Foukal, P. V., Noyes, R. W., Reeves, E. M., Schmahl, E. J., Timothy, J. G., Vernazza, J. E., & Withbroe, G. L. 1974, *ApJ*, 194, L115  
 Lites, B. W., & Skumanich, A. 1990, *ApJ*, 348, 747  
 Neupert, W. M., Epstein, G. L., Thomas, R. J., & Thompson, W. T. 1992, *Sol. Phys.*, 137, 87  
 Parker, E. N. 1974, *Sol. Phys.*, 36, 249  
 ———. 1986, in *The Sun and the Heliosphere in Three Dimensions*, Proc. of the XIXth ESLAB Symposium, ed. R. G. Marsden (Dordrecht: Reidel), 35  
 Pizzo, V. J. 1986, *ApJ*, 302, 785  
 Rottman, G. J., Orrall, F. Q., & Klimchuk, J. A. 1981, *ApJ*, 247, L135  
 ———. 1982, *ApJ*, 260, 326  
 Saba, J. L. R., & Strong, K. T. 1991, *Adv. Space Res.*, 11, 126  
 Sakurai, T. 1982, *Sol. Phys.*, 76, 301  
 Solar Geophysical Data. 1989, No. 539, 50–56  
 Uchida, Y., & Kaburaki, O. 1974, *Sol. Phys.*, 35, 451

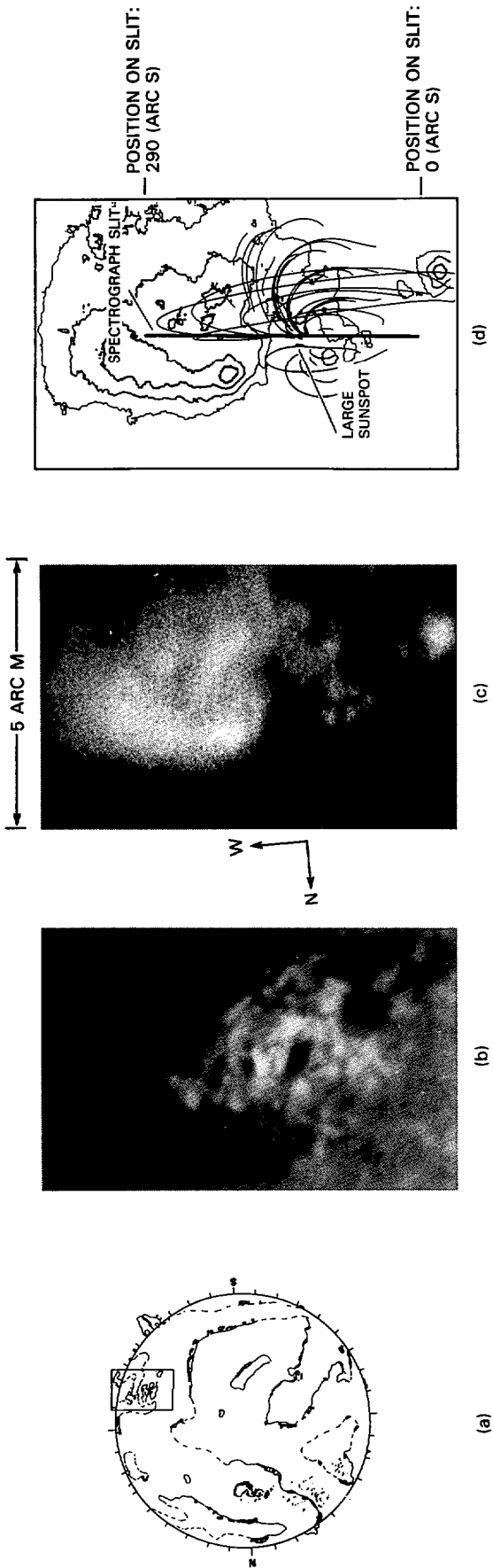


FIG. 1.—Observations made on the SERTS sounding rocket flight of 1989 May 5 were centered on NOAA Region 5464. Frame (a) shows the location of the SERTS data frame, projected on a map of photospheric neutral lines (courtesy of David Speich, NOAA). Frame (b), with an extent of  $5^{\circ} \times 8^{\circ}$ , is a centerline  $H\alpha$  filtergram of the region recorded at the Big Bear Solar Observatory. The region's large trailing sunspot, at S18 W49, is visible slightly below the center of the image. Frame (c) provides a spectroheliogram, as recorded by SERTS in Mg ix at 368.1 Å, of the same area. Frame (d) shows the position of the SERTS slit relative to the Mg ix emission isophotes during spectral observations of the region. Coronal magnetic field lines calculated from the longitudinal photospheric field using a potential code are also shown.

NEUPERT et al. (see 392, L95)